

Shedding Light on the Moisture Stability of Halide Perovskite Thin Films

Kun Sun and Peter Müller-Buschbaum*

To date, remarkable progress has been achieved in the power conversion efficiency of perovskite solar cells (PSCs). Nevertheless, the instability and degradation of PSCs under external stimuli still shadow the prospectus of their commercialization. As a notorious culprit deteriorating the stability of PSCs, moisture-induced degradation is thereby an important aspect. Herein, a comprehensive review of moisture effects on the halide perovskite film, in particular the moisture-induced degradation mechanism and methods toward enhancing the stability, is discussed. In detail, the benefits for perovskite films having a certain amount of water incorporation are elucidated, and the underlying moisture-induced structural degradation and decomposition process of perovskites are summarized. Light is also shed on the methods to enhance the moisture stability of perovskites, particularly a 3D/2D heterostructure. Thereby, this review will enlighten the readers of understanding moisture-induced degradation and the development of stable perovskites.

1. Introduction

As next-generation solar cells and in particular perovskite solar cells (PSCs) are featured with low costs, easy fabrication, and high power conversion efficiency (PCE), they have recently received tremendous interests. To date, by virtue of compositional engineering, surface passivation, and engineering the charge transport layer,^[1–4] the PCE of PSCs has reached 25.6% in champion devices.^[5] In addition, the versatile fabrication methods (e.g., slot-die coating, spray coating, doctor-blade


coating) and possibilities of applying flexible substrates enable mass production as well as novel applications (e.g., electric propulsion, solar-powered deep-space missions).^[6–8] While PSCs are on the verge of commercialization, however, the long-term stability of PSCs still remains their bottleneck in real-world applications. Perovskites tend to degrade upon exposure to external stressors (e.g., UV light, heat, humidity, oxygen), and even an inert atmosphere would induce degradation, i.e., vacuum-induced lattice shrinkage and morphology deformation.^[9] Previous studies illustrated that light exposure can break the relatively weak bonds in perovskites, leading to halide vacancy and therefore the enhancement of ion migration.^[10] In addition, heat-induced degradation results in a structural change and aggravated ion

migration in perovskites, i.e., the formation of voids and iodine and lead migration.^[11,12] To this end, understanding degradation mechanisms of perovskites under external stressors is required to enhance their long-term stability.

However, different failure mechanisms of moisture-induced perovskite degradation are raised including ion migration, phase segregation, hydration, decomposition, and others,^[13,14] which may result from the different testing conditions, perovskite compositions, fabrication methods, and so on. Therefore, we review and summarize the moisture-induced degradation mechanisms from the perspectives of structural changes and chemical decompositions. In addition, the failure mechanisms of 3D perovskites, 2D perovskites, and 3D/2D perovskites under humidity are summarized based on theoretical calculations and experimental results from the literature. We highlight the importance of surface, grain boundary, and defects of perovskites, where the moisture-induced degradation is mostly initiated and exacerbated. More importantly, the recent approaches to address the moisture instability are discussed, including compositional engineering (anion, cation, combination of anion and cation), encapsulation methods, and particularly 3D/2D heterostructures. Notwithstanding 2D perovskites may degrade in the presence of water, it can still block a moisture permeation, suppress ion migration, and reduce the defects, leading to the overall enhanced moisture resistance. We believe that when combining an encapsulation method and a 3D/2D heterostructure, the humidity instability is no longer a major constraint concerning the commercialization of PSCs. This way, PSCs will successfully make a breakthrough toward broad commercialization.

K. Sun, P. Müller-Buschbaum
TUM School of Natural Sciences
Department of Physics
Chair for Functional Materials
Technical University of Munich
James-Franck-Str. 1, 85748 Garching, Germany
E-mail: muellerb@ph.tum.de

P. Müller-Buschbaum
Heinz Maier-Leibnitz Zentrum (MLZ)
Technical University of Munich
Lichtenbergstr. 1, 85748 Garching, Germany

 The ORCID identification number(s) for the author(s) of this article can be found under <https://doi.org/10.1002/ente.202201475>.

© 2023 The Authors. Energy Technology published by Wiley-VCH GmbH. This is an open access article under the terms of the Creative Commons Attribution-NonCommercial License, which permits use, distribution and reproduction in any medium, provided the original work is properly cited and is not used for commercial purposes.

DOI: 10.1002/ente.202201475

2. Moisture Effects on Perovskites

Moisture can influence the perovskite crystallization, growth, orientation, and structure integrity from many aspects, e.g., perovskite precursor, spin coating process, and annealing steps.^[15] In this section, we focus on the benefits of water incorporation into the perovskite film and the structural degradation as well as the decomposition processes in terms of moisture-induced degradation.

2.1. Benefits of Moisture

3D perovskites are sensitive to moisture. Nevertheless, a certain level of water can be beneficial for crystal growth as well as an enhanced crystallinity, thereby giving rise to a better perovskite film quality.^[16–20] For instance, excess cesium bromide and coexistence of moisture can enhance the crystallinity of $\text{CsPbI}_{3-x}\text{Br}_x$ by promoting the transformation of the intermediate phase $\text{Cs}_{1-y}\text{Br}_y$ to $\text{CsPb}_{3-x}\text{Br}_x$ (Figure 1a,b).^[21] It was reported that the reaction between organic salts and inorganic PbI_2 frame can be accelerated by the controllable moisture treatment. As a consequence, the fast crystallization process of the intermediate perovskite film is achieved and leads to a high-quality perovskite film with significantly suppressed defects.^[22] To be noted, defects in a perovskite film can be healed during annealing at

humidity conditions, as evidenced by ex situ photoluminescence measurements.^[19] In addition, a moderate water content can also be used to regulate the structure of the perovskite film.^[23] For example, Qiao et al. uncovered that adding an optimal amount of water in the MAI solution facilitates the preferential crystal growth in the (100) plane of a sequentially deposited perovskite film, which leads to the formation of perovskite films with fewer defects.^[24] Chen et al. utilized in situ grazing incidence wide-angle X-ray scattering (GIWAXS) to monitor the perovskite film annealing at different humidity conditions and posited that incorporation of water (40% RH) during annealing enhances the texture orientation of the perovskite (Figure 1c).^[25] Moreover, moisture could provide an aqueous environment to enhance the diffusion length of mobile ions in the precursors, thereby assisting the recrystallization along with grain growth and ending up with a high-quality perovskite film with enhanced charge mobility.^[26] In addition to the 3D perovskite, water molecules also play a vital role in 2D/quasi-2D perovskite counterparts assisting crystal growth as well as suppressing 2D perovskite phases.^[27] For instance, the incorporation of water in the precursors of $(\text{BA})_2\text{MA}_4\text{Pb}_5\text{I}_{16}$ -based perovskite films imparts the modulation on the crystal orientation and phase distribution of n-value components by the formed hydration ($\text{MAI}\cdot\text{H}_2\text{O}$), resulting in the enhancement of interphase charge transfer (Figure 1d,e).^[28] Moreover, the humidity-assisted

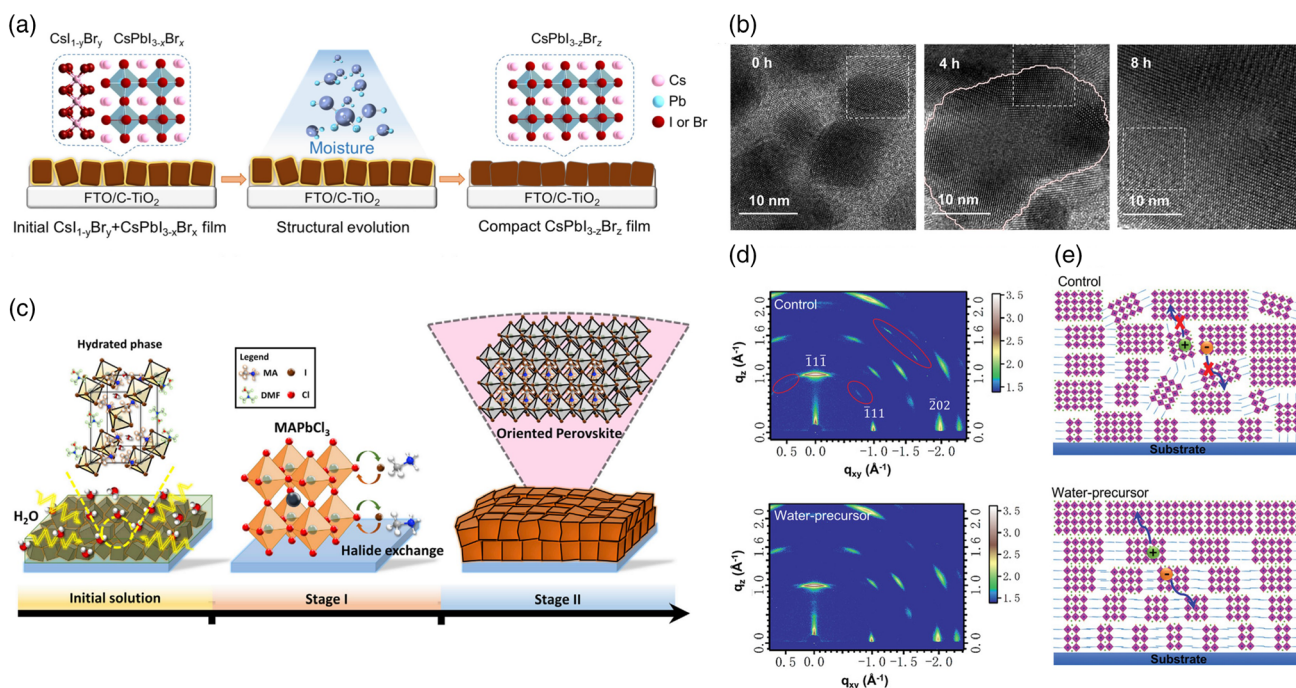


Figure 1. a) Schematic illustration of the structural evolution of the $\text{CsPbI}_{3-x}\text{Br}_x$. b) High-resolution transmission electron microscopy (HRTEM) images of $\alpha\text{-CsPbI}_{3-x}\text{Br}_x/\text{CsI}_{1-y}\text{Br}_y$ with different moisture treatment times indicated in the images, where the lattice fringes representing the $\text{CsI}_{1-y}\text{Br}_y$ are eventually vanishing after moisture treatment. Reproduced with permission.^[21] Copyright 2019, American Chemical Society. c) Schematic illustration of the structural evolution of perovskites by water treatment, where three stages include initial solution, halide exchange process, and complete formation of oriented crystals. The exchange process and the formation of hydrated phase are attributed to the water incorporation into precursor lattice and the hydrogen bond between MA^+ and H_2O molecules. Reproduced with permission.^[25] Copyright 2021, The Authors. Published by Elsevier. d) 2D GIWAXS pattern of pristine (top) and aqueous precursor-based (bottom) $(\text{BA})_2\text{MA}_4\text{Pb}_5\text{I}_{16}$ perovskite thin films. e) Schematic illustration of crystal orientation of pristine (top) and aqueous precursor-based (bottom) $(\text{BA})_2\text{MA}_4\text{Pb}_5\text{I}_{16}$ perovskite thin films, indicating the formation of oriented crystals assisted by water incorporation. Reproduced with permission.^[28] Copyright 2020, Wiley-VCH.

annealing process leads to the reduction of trap densities and facilitates the charge transfer between different 2D perovskite phases.^[29] First-principles calculations manifested that these benefits originate from the passivation of iodine vacancy by water molecules and the increased decomposition energy of 2D perovskite.

2.2. Moisture-Induced Degradation of Perovskites

An appropriate level of humidity in general increases the coverage of perovskite thin films and promotes the crystallization of perovskite crystals, thus resulting in perovskite films with a better quality. Nevertheless, excess water impairs the perovskite crystallinity and structural integrity and promotes the extraction of cation and halide out of the perovskite, whereas the water content driving the perovskite degradation is still under debate.^[30,31] For instance, 50% RH induces the formation of the nonperovskite FAPbI₃ phase and on the contrary, 60% RH has a limited impact on the structural stability of MAPbI₃.^[32,33] In this subsection, the degradation process, particularly the plausible intermediates, and degradation products of perovskites are elucidated by reviewing experimental and theoretical results.

It was reported that surface crystallographic defects, e.g., vacancy or lattice distortion, initiate perovskite degradation under humidity.^[34] Molecular dynamic calculations unraveled that MAI-terminated surfaces undergo a rapid solvation process

induced by the interactions between Pb and water molecules, whereas PbI₂-terminated surfaces are more stable under humidity. Nevertheless, the rapid dissolution of the exposed facets is exacerbated along with the formation of water-solvated Pb species after PbI₂ vacancy defects are introduced on PbI₂-terminated surfaces, suggesting that vacancy-type defects initiate and accelerate the moisture-induced degradation.^[35] Likewise, another study showed that PbI₂ vacancies can be formed during hydration, resulting from the largely reduced kinetic barrier of I⁻ migration. Apart from PbI₂ vacancies, point defects such as I and MA vacancies are also easily formed in the hydration process in comparison to the formation of MAI vacancy. These defects, in turn, create deep transition levels, resulting in the degradation of perovskites.^[36] In addition, it is reported that the halide vacancy at the perovskite surface can trap the migrated I⁻ and Br⁻ with the help of water, leading to Br-rich and I-rich phases. As such, the moisture-induced phase segregation is likely taking place with the aid of halide vacancies and ion migration.^[37] Moreover, the moisture was found to initiate perovskite degradation at the atmospheric interface and then move to the grain boundary,^[38–40] in which the grain boundary contains an amorphous intergranular layer (Figure 2a) allowing the fast penetration of moisture into the perovskite films.^[41] With the further uptake of water into perovskite film, the degradation expands toward the grain interiors along the in-plane direction (Figure 2b–d),^[39,41] accompanied by a slight expansion of the

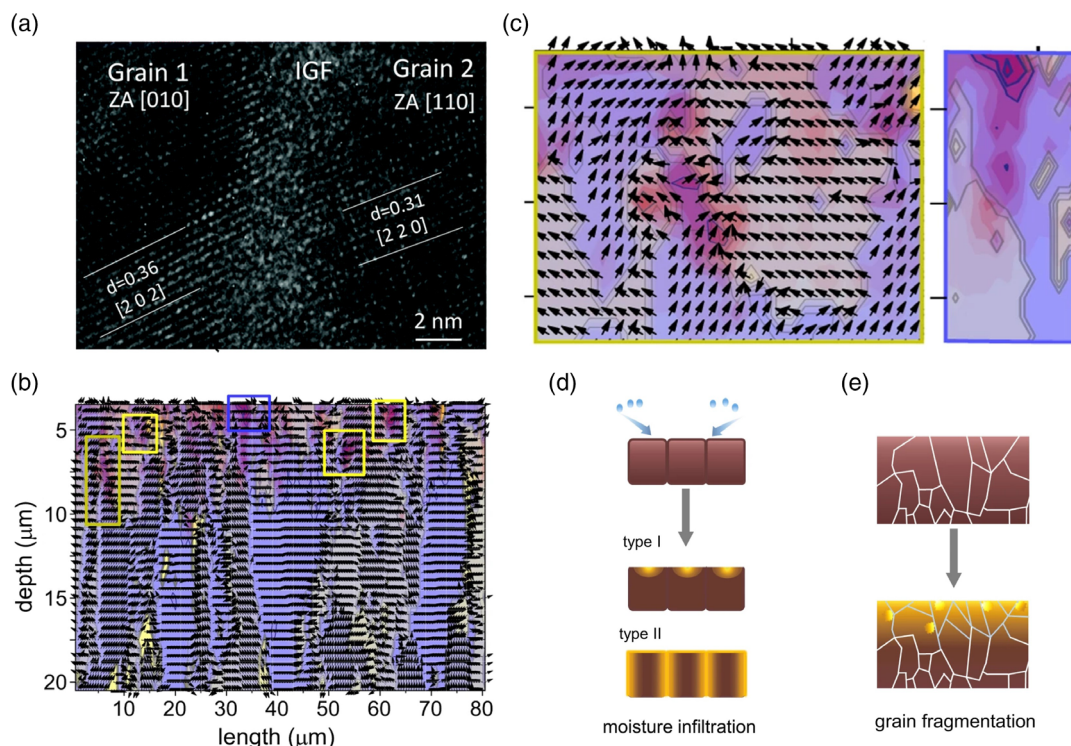


Figure 2. a) HRTEM cross-sectional image showing the amorphous intergranular film between two adjacent grains, where the lattice and grain are indexed based on the simulation results of diffraction patterns. Reproduced with permission.^[41] Copyright 2017, Royal Society of Chemistry. b) Overlap between the orientation map of (100) perovskite peak and the intensity map of PbI₂, where the blue and yellow boxes represent the moisture-induced perovskite degradation at the grain surface and boundary, respectively. c) Magnified image of (b). Schematic illustration of d) moisture propagation path and e) grain fragmentation at the degradation region. Reproduced with permission under the terms of the Creative Commons CC BY license.^[39] Copyright 2022, The Authors. Published by Springer Nature.

grains,^[42] or the formation of a large cluster with the adjacent grains.^[32] In addition, the water-induced degradation can also lead to the grain fragmentation (Figure 2e), resulting from the tensile strength in the top region.^[39] The tensile strength originates from the annealing process where the top surface of the film cools down faster than other film regions, and in turn accelerates the degradation and provides the driving force for crystal fracture.^[43] It is also worth mentioning that the degradation rate is sensitive to the grain size, with smaller crystals being more affected.^[41,42]

Researches on the moisture-induced decomposition of perovskite, in particular MAPbI₃, have been well studied. In general, water can easily penetrate into perovskites due to the lower absorption energy (≈ 0.3 eV),^[44] and be regarded as a catalyst to induce perovskite hydration and even decomposition. For instance, Kelly et al. reported that the formation of a hydrated intermediate phase (CH₃NH₃)₄PbI₆·2H₂O is the first step of moisture-induced degradation (Equation (1)), as evidenced by the in situ Grazing incidence X-ray diffraction (GIXRD), where

the formation of hydrate phase is likely attributed to the hydrogen bonds of H₂O and CH₃NH₃⁺.^[45] In addition to the (CH₃NH₃)₄PbI₆·2H₂O hydrate, another degradation product of monohydrate MAPbI₃·H₂O (Equation (1)) was found under high humidity environment (80% RH), along with the additional grain boundaries.^[46,47] Likewise, our previous work also revealed that moisture induced the formation of metastable hydrate phases along with the domain swelling (Figure 3a), thus giving rise to the round and pebble-like crystals (Figure 3b).^[42] The moisture-induced hydration process is always accompanied by the structure change from 3D crystals to 1D structure and 0 D framework.^[48] With a numerical model simulating the water diffusion process in the perovskite structure, Xu et al. proposed that a certain level of structural imperfection initiates the degradation assisted by the collapse of the perovskite into 1D chains.^[49] This hydration transformation process is independent of film thickness because water molecules propagate along the grain boundary and in-plane direction.^[41,48] Moreover, the hydration process is also partially reversible upon storage in

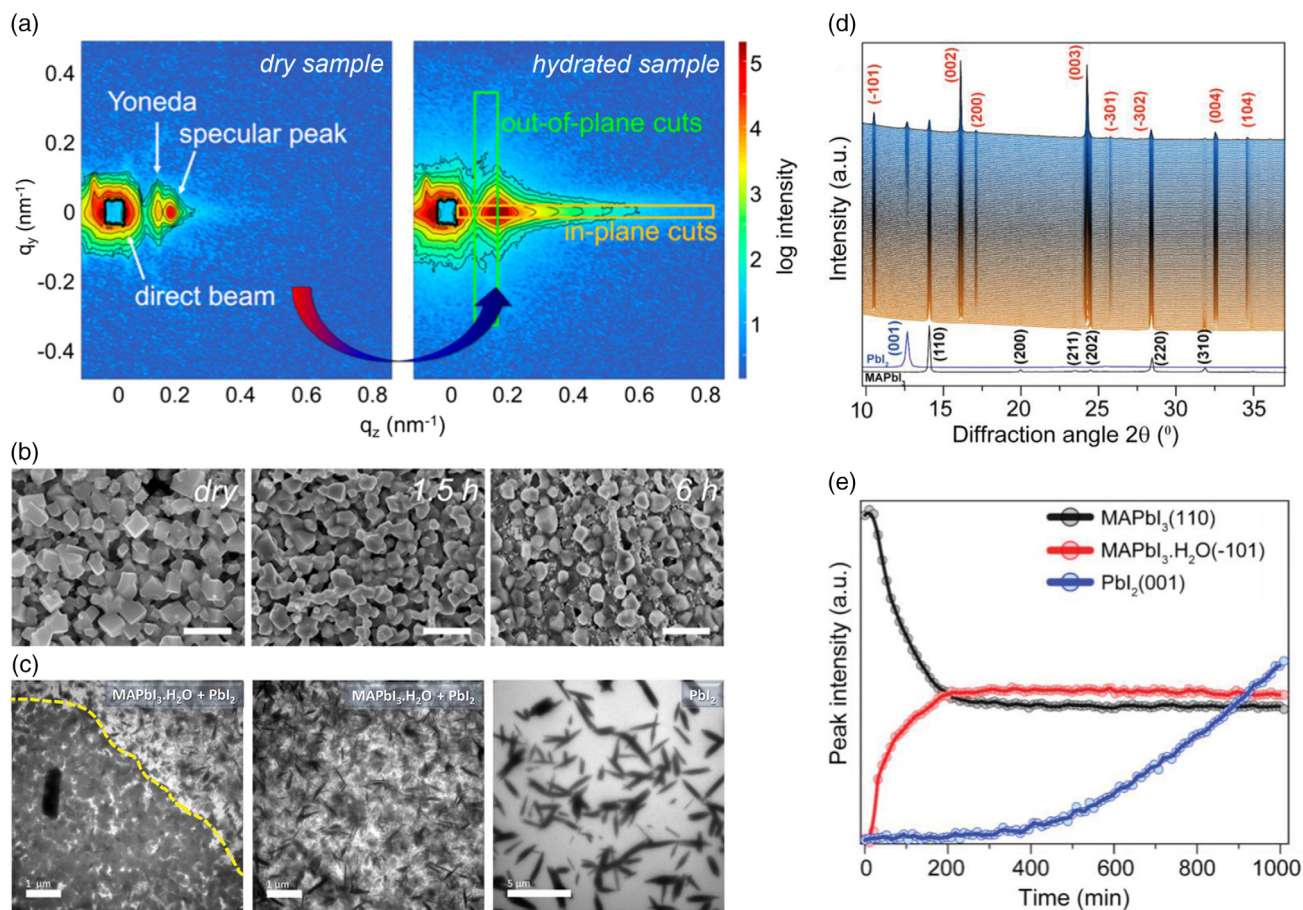
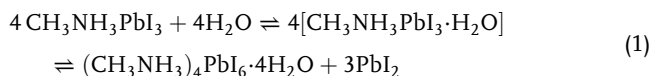
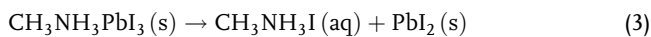
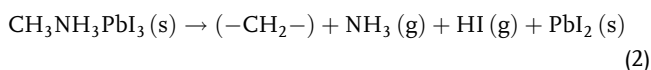


Figure 3. a) Water uptake seen in representative 2D GISANS data with direct beam, specular beam, Yoneda peak, and cut position being marked. The scattering intensity is enhanced and the Yoneda peak shifts to the specular position after D₂O permeation. b) A dry MAPbI₃ film and films after 1.5 and 6 h exposure to D₂O vapor, where the faceted crystals become round-shaped during hydration. Reproduced with permission.^[42] Copyright 2018, American Chemical Society. c) In situ TEM images of morphology evolution from MAPbI₃ to PbI₂. d) Contour in situ X-ray diffraction (XRD) plot of MAPbI₃ film versus time under 85% RH, where the characteristic peaks are indicated in the image. e) The peak intensity evolution over time, where the black, red, and blue represent the (110) plane of MAPbI₃, (101) plane of MAPbI₃·H₂O, and (001) plane of PbI₂, respectively. Reproduced with permission.^[53] Copyright 2020, Wiley-VCH.

vacuum or in low RH, which, in turn, indicates the formation of $\text{CH}_3\text{NH}_3\text{PbI}_3$ hydrate.^[42,46,50]



Further uptake of water fractures the hydrogen bonds between the organic cation and metal or halide ion and forms new hydrogen bonds with perovskites, leading to the high-mobility ions.^[51] For instance, a hydrolysis reaction of MAPbI_3 is taken place in the moisture environment and gives rise to the PbI_2 and aqueous MAI, and at last volatile compound CH_3NH_2 and HI (Equation (2) and (3)).^[30,52] In another case, Sauvage et al. proposed that there are two stages in terms of moisture-induced degradation. First, the formation of monohydrate $\text{MAPbI}_3 \cdot \text{H}_2\text{O}$ (Figure 3c) and the corresponding disappearance of MAPbI_3 after 200 min exposed to 85% RH. Second, the growth of decomposition product (PbI_2) of $\text{MAPbI}_3 \cdot \text{H}_2\text{O}$ starts accelerating in particular after 400 min (Figure 3d,e).^[53] Interpretations of MAPbI_3 under humidity contrary to the abovementioned degradation process are referred to literatures.^[54,55]



Analogous to the MAPbI_3 perovskites, mixed cation/halide perovskites also tend to degrade and decompose in the presence of water.^[38,56–58] For example, the formation of PbI_2 and PbBr_2 of MAPI , $\text{FA}_{0.83}\text{MA}_{0.17}\text{Pb}(\text{I}_{0.83}\text{Br}_{0.17})_3$, and $\text{FA}_{0.83}\text{Cs}_{0.17}\text{Pb}(\text{I}_{0.83}\text{Br}_{0.17})_3$ under 90% RH was revealed by time-of-flight grazing incidence small-angle neutron scattering.^[59] On the other hand, moisture can induce phase segregation of mixed halide perovskites.^[60,61] Sauvage et al. discovered a new phase of mixed halide perovskite by in situ XRD (Figure 4a), manifesting the phase segregation after exposure to humidity.^[14] In terms of the tin-based halide perovskites under humidity, Kaiser et al. compared the moisture stability of MAPbI_3 , MASnI_3 , and DMASnBr_3 through ab initio molecular dynamics simulations (AIMD). The facile solvation of surface tin–iodine bonds results in the fast decay of MASnI_3 , whereas MAPbI_3 remains robust in the presence of water molecules (Figure 4b). By contrast, the amorphous surface layer of hydrated 0 D SnBr_3 complexes acts as a shield layer and thus protects the inner structure of DMASnBr_3 from degradation (Figure 4b).^[62]

Likewise, inorganic perovskites suffer from moisture instability as well, particularly phase transitions triggered by humidity. It was found that CsPbI_3 undergoes a phase transition from a high-temperature cubic phase to a low-temperature orthorhombic phase under humidity (Figure 4c,d).^[63,64] Through thermodynamic calculations, another possible degradation mechanism of CsPbI_3 was raised by Rubel et al. that CsPbI_3 is dissolved in water, resulting in the formation of Cs^+ , I^- , and PbI_2 (Equation (4)).^[52] The absorbed water molecules can generate vacancies in the crystal lattice and lower the energy barrier of phase transition, thus aggravating the moisture-induced phase transition.^[65] Notably, the reduction of free-energy barrier of halide vacancy leads to a large enhancement of the transition

rate.^[66] In addition, free-energy calculations illustrated that the increased halide vacancies under humidity can be ascribed to the large solvation enthalpy of halide ions and their corresponding lower formation energy.^[67] Likewise, in the case of CsPbI_3Br being exposed to humidity, the degradation is attributed to the phase transition from perovskite α phase to nonperovskite δ phase.^[68] It is worth mentioning that there is a slight distortion of interatomic distances in the top layer of $\gamma\text{-CsPbI}_3$ (220) perovskite surface in the presence of water molecules, whereas a large distortion is observed in the MAPbI_3 surface. This behavior manifests that water molecules are prone to interact with MAPbI_3 surface in comparison to the $\gamma\text{-CsPbI}_3$ surface, as evidenced by the first-principles calculations.^[69] To wrap up, moisture-induced phase transition in inorganic perovskites is fundamentally different from the degradation process of hybrid perovskite MAPbI_3 , where the hydration and decomposition process of MAPbI_3 under humidity have been described above.



2D perovskites, derived by isolating the corner-sharing PbI_6 octahedra sheets with bulky organic cations, have been proven to exhibit superior stability and water resistance in comparison to their 3D counterparts.^[70,71] Nevertheless, evidence shows that 2D and quasi-2Ds degrade in the presence of moisture, and give rise to different degradation products under different conditions. For instance, Jin et al. proposed that large- n phases of $(\text{PEA})_2(\text{MA})_{n-1}\text{Pb}_n\text{I}_{3n+1}$ ($\text{PEA} = \text{C}_6\text{H}_5\text{C}_2\text{H}_4\text{NH}_3^+$) directly degraded into $n=1$ phase and MAI and PbI_2 under 85% RH.^[72] In contrast to the aforementioned degradation process, a structural transformation from 2D/quasi 2D layered perovskite to 1D perovskite-like chains and, to the end, the formation of PbI_2 were detected.^[73] The variations in degradation products can be likely attributed to the different film composition, fabrication methods, film quality, and testing protocols (e.g., relative humidity, vacuum, and inert gas).^[15,74] In addition, the interaction between uncoordinated defects and water molecules should also be taken into account in terms of moisture-induced 2D/quasi-2D degradation.^[75] Moreover, 3D/2D perovskites experience rapid disproportionation under humidity, i.e., transformation from quasi-2D perovskite with higher n phase into relatively stable lower n 2D perovskite (Figure 5a,b).^[76,77] However, they disclosed that 2D perovskite inhibits the formation of PbI_2 , manifesting the suppression of MA^+ and I^- ion migration. More recently, Bach et al. introduced the 2D perovskite layer on top of 3D layer to enhance the stability; however, they discovered that the 2D perovskite decompose into BAI and 3D perovskite after aging under 85% RH for 5 days, as revealed by XRD measurements. The decomposition is ascribed to the crystals imperfection and structural defects, resulting from the rapid crystal formation.^[71]

In the case of synergistic effects of humidity and other stressors, perovskites degrade even faster. For instance, the elevated temperature and light illumination result in perovskite rapid degradation, resulting from the formation of additional recombination centers.^[78] Recently, a study revealed that $\text{FA}_{0.85}\text{Cs}_{0.15}\text{PbI}_3$ experiences a phase separation ($\delta\text{-CsPbI}_3$, $\delta\text{-FAPbI}_3$, PbI_2) and the evaporation of FA^+ under light and humidity, while no

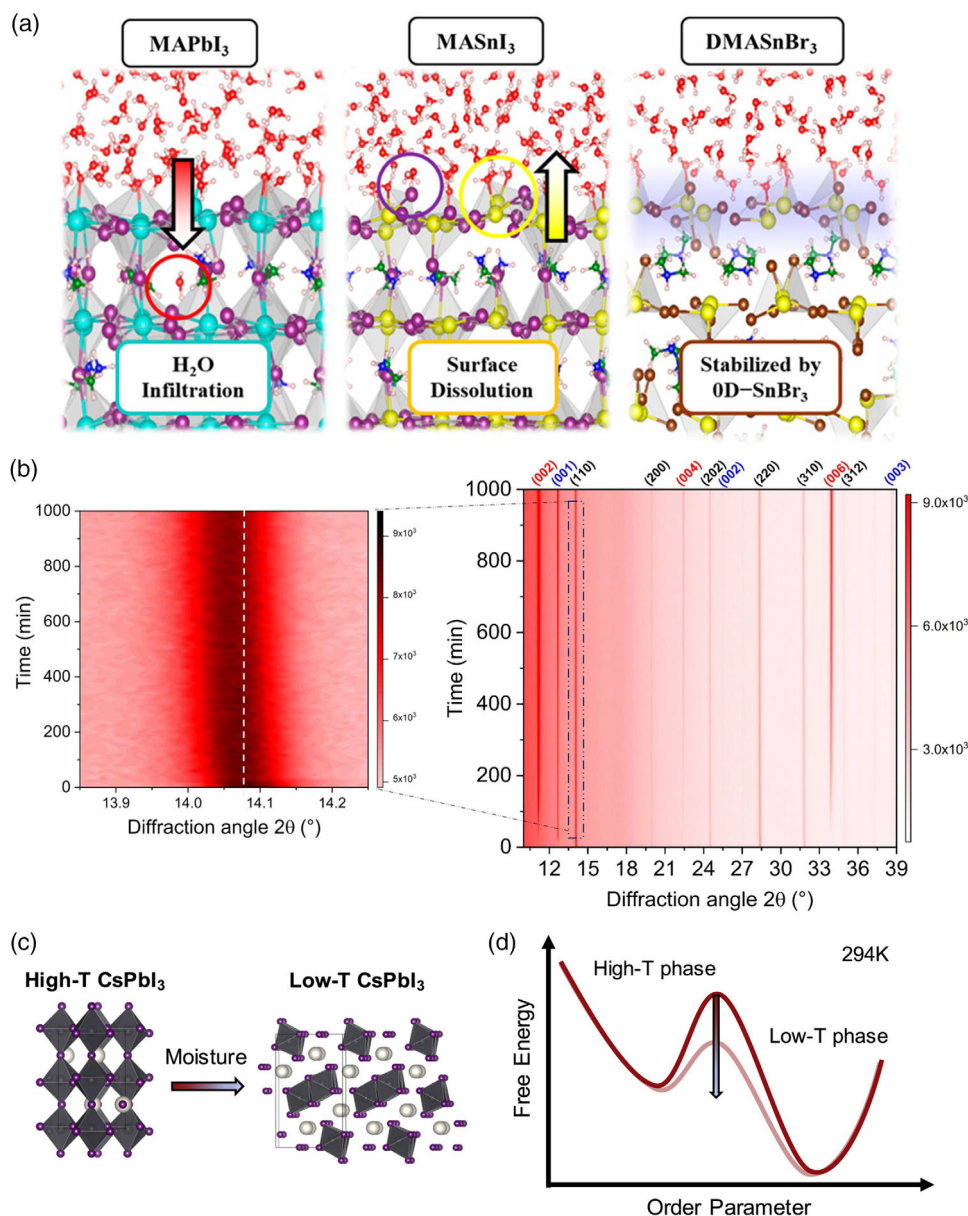


Figure 4. a) Ab initio molecular dynamics simulations of MAPbI₃, MASnI₃, and DMASnBr₃, manifesting water permeation into the MAPbI₃ structure, the surface dissolution of MASnI₃, and the formation of hydrated 0D SnBr₃ complexes under humidity. Reproduced with permission under the terms of the Creative Commons CC BY license.^[62] Copyright 2022, The Authors. Published by American Chemical Society. b) Contour in situ XRD pattern of CsMAFA film under 85% RH versus time, where the black, blue, and red crystallographic orientations correspond to the CsMAFA perovskite, PbI₂, and segregated CsPb₂Br₅, respectively. The left image represents the zoom-in evolution of (110) diffraction peak of CsMAFA upon exposure to humidity. Reproduced with permission.^[14] Copyright 2022, Zhengzhou University. Published by John Wiley and Sons. c) Schematic illustration of moisture-induced phase transformation from high-T CsPbI₃ (left) to low-T CsPbI₃ (right), where the white, gray, and purple atoms denote cesium, lead, and iodine, respectively. d) Illustrative energy diagram of CsPbI₃ (red curve) in comparison to common moisture-induced modification (faint red curve) of the energy scheme, manifesting the lowered phase transformation barrier after water incorporation. Reproduced with permission.^[64] Copyright 2021, Elsevier.

decomposition and change in the spatial change of FA upon exposure to either light or moisture alone.^[79]

Despite tremendous efforts that have been devoted to the stability-related investigations, the absence of unified measuring protocols leads to discrepancies in the degradation rate and product. Therefore, to have reproducible and comparable results, we recommend researchers to investigate the failure mechanism

under ISOS protocols.^[80] In light of the reversible hydration process and degradation rate of perovskites,^[81] real-time characterization methods are required and prioritized to have a full picture of the degradation process.^[82] In particular, we highlight the usage of in situ grazing incidence X-ray scattering techniques, which feature short measurement times, a large probed sample area, and good statics,^[83–86] thereby enabling the precise and full

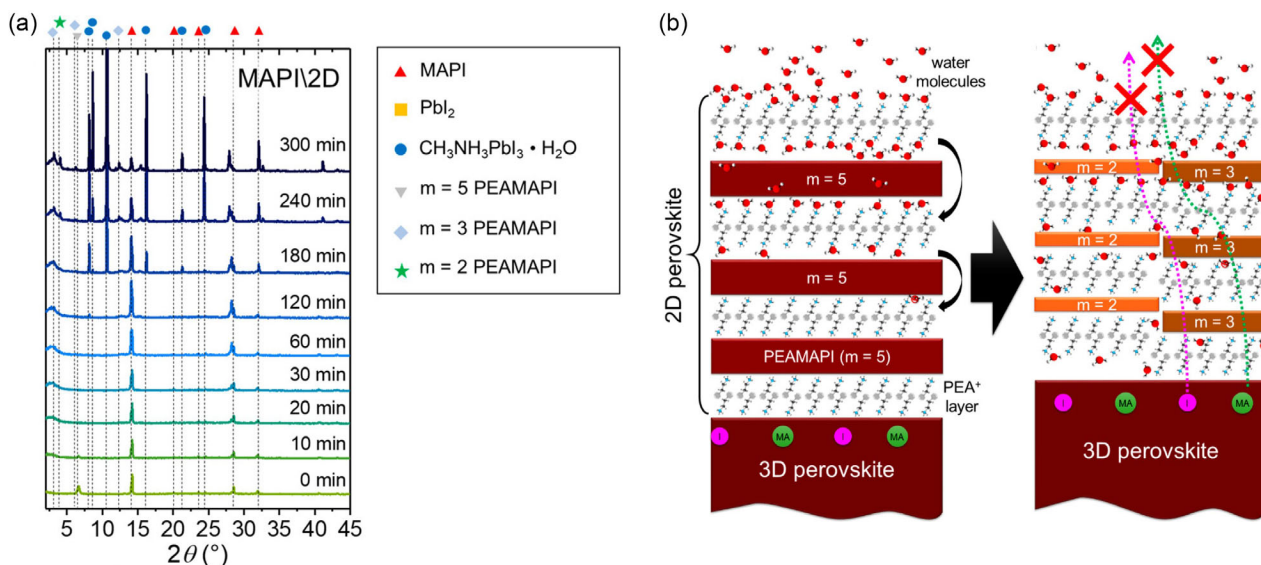
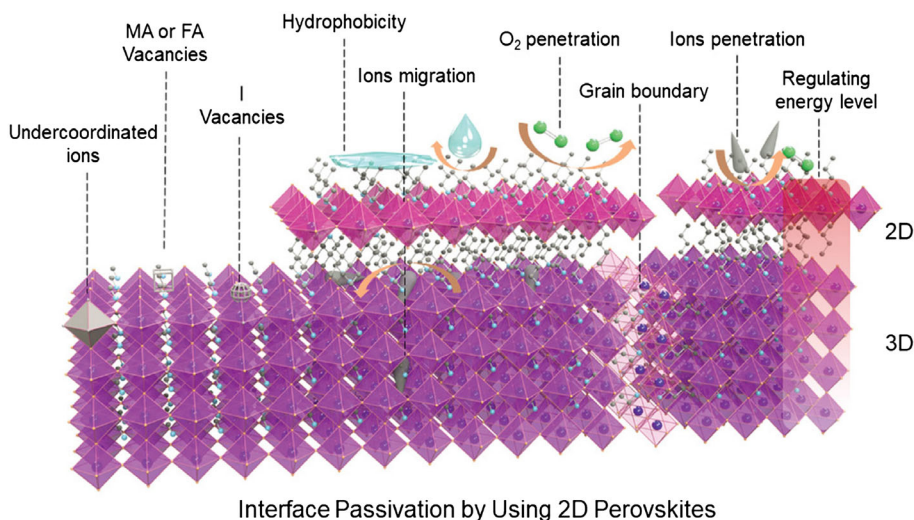


Figure 5. a) In situ XRD patterns of MAPbI₃/2D thin film under 90% RH, where the characteristic peaks are labeled with different symbols, as indicated in the image. b) Schematic illustration of moisture-induced degradation of 3D/2D thin film. The left image shows the intact 3D/2D heterostructure, whereas the right image suggests the disproportionation of $m = 5$, 2D perovskite (m refers to the number of inorganic sheets) into MAPbI₃ and more stable 2D perovskite with $m = 2, 3$ phases. The resulted 2D perovskites with $m = 2, 3$ phases impede the I⁻ and MA⁻ diffusion, and thus further decomposition to PbI₂ and volatile compound. Reproduced with permission.^[76] Copyright 2019, American Chemical Society.



Interface Passivation by Using 2D Perovskites

Figure 6. Schematic illustration of the surface passivation by 2D perovskites, in which the possible functionalities of 2D perovskite are illustrated. Moreover, the 2D capping layer on top of 3D layer can block water penetration. Reproduced with permission.^[136] Copyright 2022, Wiley-VCH.

detection of perovskite growth and degradation.^[83,87] When using neutrons instead of X-ray, due to the contrast enhancement via deuteration of the water, in particular the water distribution inside the perovskite films can be traced.^[39,73]

3. Strategies to Enhance Moisture Stability

In this section, we summarize the methods of enhancing the moisture stability of perovskites, including composite engineering, encapsulations, and in particular formation of 3D/2D heterostructure. We highlight the combination of 2D and 3D

perovskite for the following reasons (**Figure 6**): 1) Defects such as MA/FA/I/Pb vacancies and uncoordinated lead halide clusters can be formed in the fabrication process,^[88–90] along with cracks and pinholes during crystallization, which initiate the degradation of perovskites upon exposure to humidity. 2D perovskite can fill in these vacancies, interact with uncoordinated ions, and embed in the cracks, grain boundaries, and pinholes in the film,^[91,92] thereby eliminating defects and promoting the quality of perovskite films; 2) Intrinsic instability and instability under external stressors of the perovskite still limit its application in the real world. Given the rather low formation energy and

small radius of MA and FA cations, it is easy for them to escape from the perovskite lattice under external stimuli. In addition, 3D perovskites are vulnerable to humidity, as discussed in the previous section. In this regard, as a blocking layer on top of 3D perovskite layer, 2D perovskites can prevent the invasion of external stressors and suppress ion migration, arising from the hydrophobicity as well as the large formation energy.^[93]

3.1. Composite Engineering

The vacancies such as organic cation and halide vacancies, with lower formation energy,^[94] are normally located on the surface or grain boundary of perovskites and are prone to diffuse into the interior of the crystals. With being exposed to external stimuli, the degradation is initiated at these sites and aggravated within the whole crystal, thus resulting in the decomposition of the perovskites. Composite engineering, in this perspective, has shown to be an important strategy to reduce the inherent vulnerability of perovskite with respect to external stimuli, i.e., partially or completely replacing the anions/cations. For instance, Bach et al. revealed that doping Rb^+ and K^+ into $\text{Cs}_{0.05}\text{FA}_{0.79}\text{MA}_{0.16}\text{PbI}_{2.49}\text{Br}_{0.51}$ /BAI 3D/2D perovskites gives rise to high crystallinity, better film morphology, and superior moisture resistance, which, in turn, enhances the PSCs performance and stability under humidity and heat (85 % RH, 85 °C).^[71] The introduction of organic bulky cation can be, on

the other hand, applied to enhance the perovskite stability against humidity. Phenethylammonium was utilized to partially substitute MA^+ in MAPbI_3 and found to be beneficial for obtaining perovskites with large crystal sizes and less trap densities. As a result, the PSCs retained 75% of initial performance storage under $50 \pm 10\%$ RH for 30 days.^[95] In addition, MAPbI_3 perovskites with acetamidinium (AA) substitution exhibited remarkable moisture resistance (Figure 7a) and carrier lifetime under ambient exposure ($72 \pm 3\%$ RH), which is due to the strengthened electrostatic interaction and stabilized AA cation inside the perovskite matrix.

It was reported that water and oxygen-induced perovskite degradation is exacerbated at the vacancy sites. Employing anion engineering to partial substitution of halide with other anions can reduce defects and thus alleviate the perovskite degradation.^[96] For example, thiocyanate (SCN^-) can greatly enhance the stability of perovskites by reducing the formation of I^- vacancies.^[30] This is due to the stronger interaction between Pb_2^+ and SCN^- compared to the bond of I^- and Pb_2^+ , resulting from the strong bond between lone pairs from atom S and N and Pb ions.^[97,98] In addition to SCN^- , acetate ions (OAc^-) is also in favor of enhancing the stability of perovskites, which was achieved by the high crystallinity and the reduction of uncoordinated Pb after the substitution of Cl^- with OAc^- . As a consequence, the PCE of $\text{MAPbCl}_{3-x}(\text{OAc}^-)_x$ -based PSCs maintained 84% of its initial PCE after 800 h operated at 70% RH.^[99]

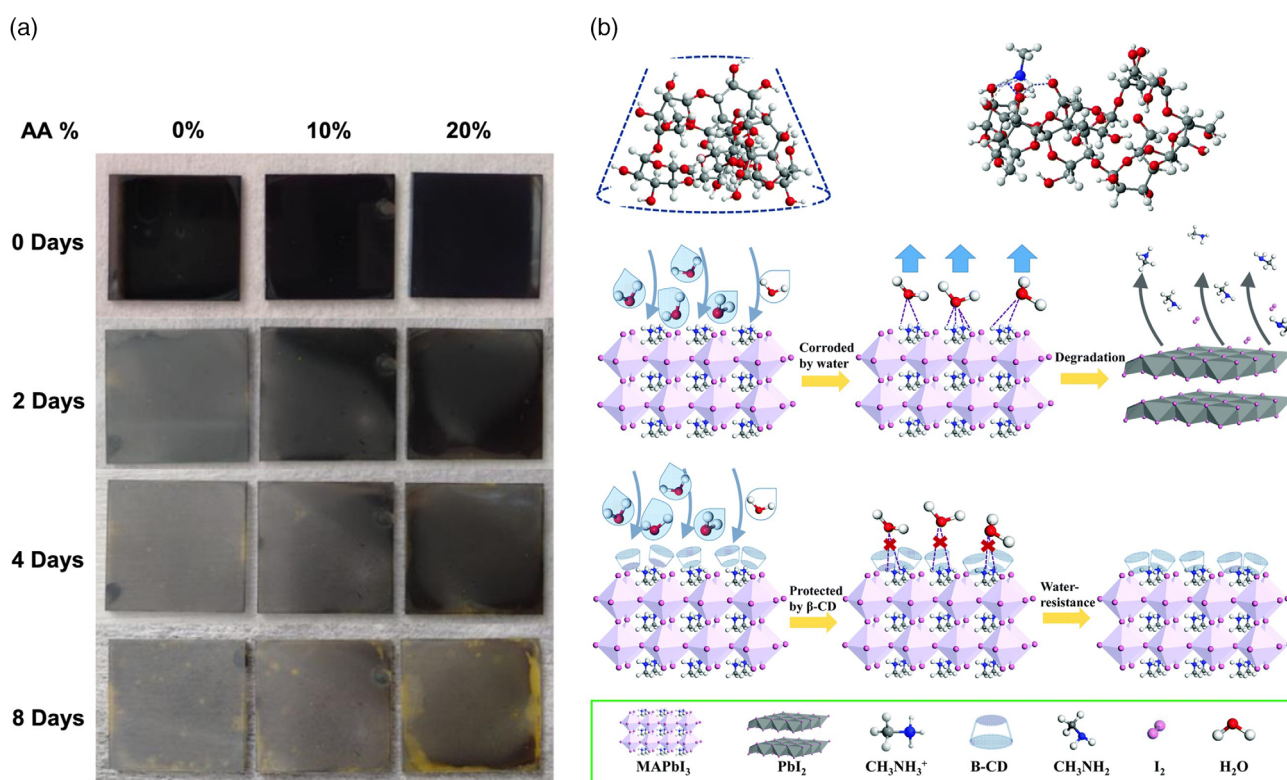


Figure 7. a) Stability of MAPbI_3 with different amounts of AA substitution at 85 °C and 75% RH. Reproduced with permission.^[137] Copyright 2020, American Chemical Society. b) The top left and right images show the molecule structure of β -cyclodextrin molecules and the interaction of perovskites with β -cyclodextrin. The middle and bottom images illustrate the moisture-induced degradation mechanism of pristine MAPbI_3 and the working principle of β -cyclodextrin. Reproduced with permission.^[111] Copyright 2018, Royal Society of Chemistry.

Likewise, Pan et al. utilized superhalogen BH_4^- to partially replace I^- , and they found that the superhalogen BH_4^- can reduce the defects and enhance the film quality. Such an effect is related to the compensation of iodine vacancies with BH_4^- substitution and its interaction with methylamine molecules by dihydrogen bonding. Therefore, a hysteresis-free $\text{MAPbI}_{3-x}(\text{BH}_4^-)_x$ device preserved 90% of the initial PCE upon exposure to $50 \pm 10\%$ RH for 1200 h.

In addition to A and X site modification, doping and substitution of the B site is an alternative way to enhance humidity resistance of perovskite materials. However, there are only a few studies focusing on the substitution of B sites because both structural and energetic requirements need to be fulfilled. The valence band is constituted of p orbitals of halide anions and s orbitals of B site cations, while the conduction band is formed by the p orbitals of B site cations.^[100] In other words, the substituted elements need to fulfill the abovementioned condition to form a suitable band alignment, which, in turn, limits the candidates of B site substitution. DFT calculations suggest that Ge and Sn doping is the most promising strategy among all other B cations (e.g., Mg, Zn, Cd) to enhance stability while achieving desired bandgaps.^[101] Additionally, by scanning Kelvin probe microscopy, Hsieh et al. found that the adhesion of Sn-doped perovskite thin films is much lower compared to that of pure perovskite thin film (CsPbBr_3), indicating that Sn-doped perovskite thin films exhibit higher water resistance under 75% RH condition.^[102] In addition, Ni has stood out to enhance the moisture resistance of perovskite materials, resulting from the improved integrity and short-range order of the crystal lattice with Ni incorporation. Such integrity is attributed to the strong preference of Ni ions for octahedra coordination with halide ions, which, in turn, eliminates the halide vacancy. As a result, devices retained 90% of initial efficiency after storage under 10–20% RH for 800 h.^[103] It should be pointed out that local lattice strain facilitates the formation of defects, which is the major source inducing perovskite degradation under humidity. By incorporating selected B-site dopants (e.g., Cd), the lattice strain can be relaxed

and the formation energy of defects is concurrently increased. As such, PSCs reserved 90% of their initial efficiencies after 30 days of storage at 50% RH.^[34]

In addition, recent studies illustrate that combing anion and cation engineering largely promotes the hydrophobicity and quality of perovskite films, therefore leading to the enhancement of moisture resistance. For example, CsPbI_2Br perovskites exhibited an excellent water resistance up to 100 h immersing into water, arising from the reduced crystal defects as well as improved crystallinity.^[104] Likewise, by carefully tuning the crystal growth, Li et al. demonstrated a high-quality CsPbI_2Br film with robustness against moisture, oxygen, and UV light.^[105] In summary, point defects (e.g., V_{I} , V_{MA}) with relatively lower formation energy are shown to initiate or accelerate perovskite degradation because of their affinity to water molecules. The local lattice strain exacerbates the formation of defects, while composition engineering has shown to be an effective way to address moisture instability of perovskites by relaxing the lattice strain and suppressing the defects formation.

To retrieve the long-term tolerance of perovskites, various functional molecules such as hydrophilic polyvinyl alcohol (PVA) and 2-aminoethanethiol (2-AET) were introduced into perovskite film.^[106,107] Functional molecules can directly enhance water resistance by interacting with water molecules,^[108] or indirectly by regulating nucleation and crystallization and passivating the defects.^[109,110] For example, doping β -cyclodextrin (β -CD) into the perovskite precursor was demonstrated to facilitate the crystallization and enhance the stability against humidity, which was attributed to the supermolecule interaction with organic cation by hydrogen bonding (Figure 7b).^[111] Additionally, the incorporation of 1,2-bis(chlorodimethylsilyl)ethane (Si-Cl) molecules was shown to be an effective method to alleviate water erosion in terms of the inorganic perovskites (CsPbI_3). The Si-OH solid protection was achieved by the chlorinated CsPbI_3 with a hydrolysis product of hydrogen chloride (HCl), improving the crystallization and phase stability.^[112]

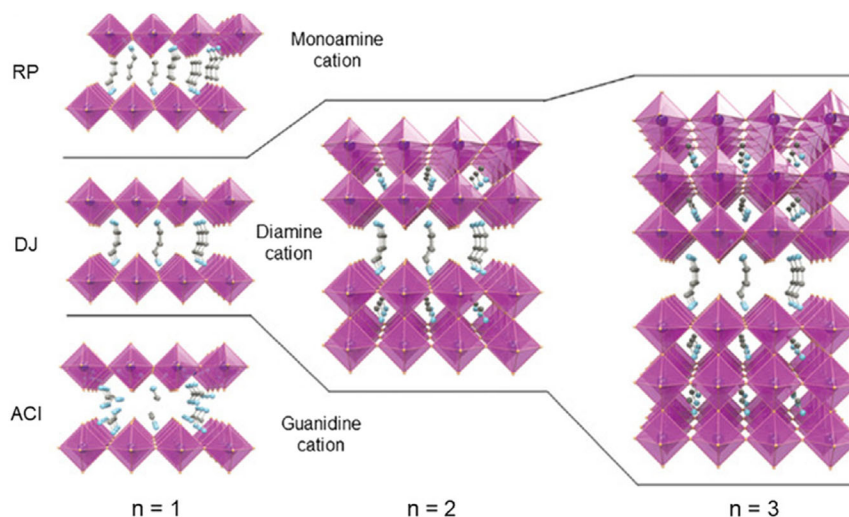


Figure 8. Schematic illustration of 2D and quasi-2D perovskites, including RP, DJ, and ACI crystal structure. Reproduced with permission.^[136] Copyright 2022, Wiley-VCH.

3.2. 3D/2D Heterostructure

2D layered perovskites (Figure 8), in which inorganic sheets are separated by organic bulky cations, have recently attracted significant interests because of their superior stability, in particular stability against humidity.^[113] In general, 2D perovskites can be divided into three types, namely, Dion–Jacobson (DJ), Ruddlesden–Popper (RP), and altering cations in interlayer (ACI) space perovskites. RP and DJ perovskites have general formulas of $(A')_2A_{n-1}B_nX_3X_{n+1}$ and $A''A_{n-1}B_nX_3X_{n+1}$, respectively, in which A' and A'' represent the monovalent bulky cation (e.g.,

aliphatic or aromatic-based cation) and divalent organic spacers, A is organic cation in inorganic slabs, and n refers to the number of $[PbI_6]_4^-$ octahedra layer.^[114]

Considering the superior water resistance of 2D perovskite, it is feasible and reasonable to combine 2D perovskite with 3D perovskites. Many attempts have been devoted to enhance both PCE and the stability of 3D perovskites using 2D perovskites, e.g., mixing a 2D solution with 3D precursors or forming a 2D/3D heterostructure.^[115–117] For example, Snaith et al. introduced *n*-butylammonium (BA) cations into a $FA_{0.83}Cs_{0.17}Pb(I_\gamma Br_{1-\gamma})_3$ 3D perovskites and the corresponding

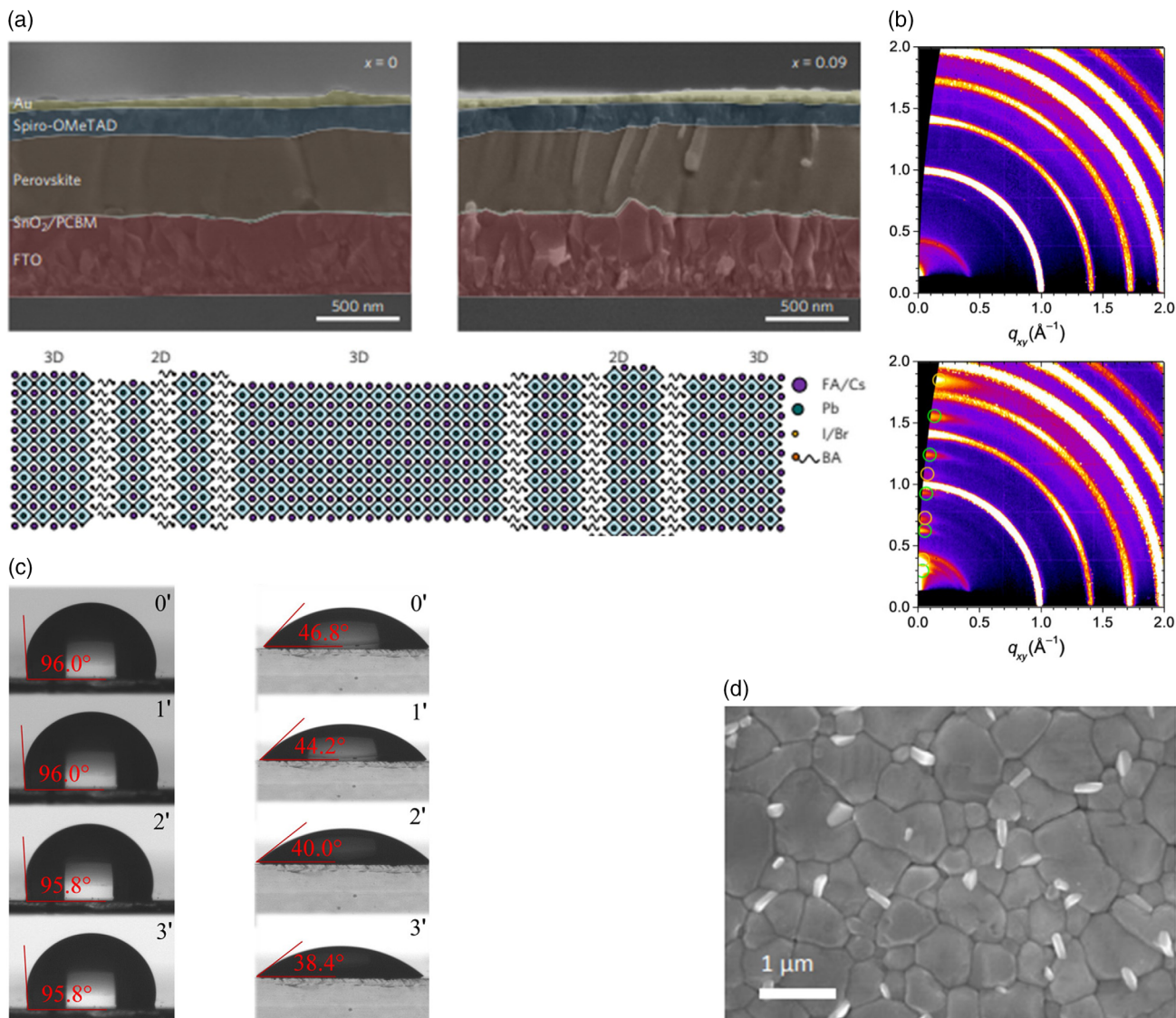


Figure 9. a) Cross-sectional images of $FA_{0.83}Cs_{0.17}Pb(I_{0.6}Br_{0.4})_3$ (top left) and $BA_{0.09} (FA_{0.83}Cs_{0.17})_{0.91}Pb(I_{0.6}Br_{0.4})_3$ devices (top right), where the bottom illustration shows the self-assembled 2D/3D heterostructure. Reproduced with permission.^[118] Copyright 2017, Nature Publishing Group. b) 2D GIWAXS patterns of $FAPbI_3$ film (top) and $FAPbI_3/FEAI$ film (bottom), in which the green and orange circles indicate the β and γ phases of 2D perovskites, respectively. c) Contact angle measurement of water droplet on the surface of 3D/2D (left) and 3D perovskite film (right) with timeline indicated, manifesting the excellent moisture stability of 3D/2D perovskite. Reproduced from [138]. Copyright 2019, The Authors, some rights reserved; exclusive licensee AAAS. Distributed under a Creative Commons Attribution NonCommercial License 4.0 (CC BY-NC). d) Scanning electron microscopy (SEM) image of $FAPbI_3/PEA_2PbI_4$ film, indicating that 2D perovskite is located at the grain boundary. Reproduced with permission under the terms of the Creative Commons CC BY license.^[120] Copyright 2018, The Authors. Published by Springer Nature.

devices sustained 80% of their original efficiency under 40–50% RH. The formation of 2D perovskite platelet, which is interspersed between 3D perovskite grains (Figure 9a), leads to the suppression of nonradiative charge recombination and thus the enhanced stability.^[118] In addition, with the addition of $C_6H_{18}N_2O_2PbI_4$ (EDBEPbI₄) microcrystals into 3D perovskite solutions, the grain boundaries are passivated by the formed phase-pure 2D perovskites, thus boosting the PCE and the stability against moisture.^[115] In terms of 2D/3D stack, recently a 2D/3D heterostructure layer containing FABr-doped 4-fluorophenethylammonium iodide (4FPEAI) 2D perovskite layer was achieved, which largely boosts the humidity resistance and PCE of 3D perovskite. Such enhancement is ascribed to the better formation of 2D capping layer and the grain boundaries passivation.^[119] In addition, the smaller organic cations and halogens with lower activation energy can easily migrate under external stimuli and cause perovskites degradation. In this perspective, a 2D perovskite layer is expected to mitigate the ion migration due to the insulating bulky organic cation. Table 1 lists the 2D perovskites used, 3D perovskite composition, and the corresponding stability against humidity by doping 2D solutions into 3D precursors and forming the 3D/2D heterostructure. Recently, a 2D perovskite layer containing a pentafluorophenethylammonium (FEA) cation was introduced on top of 3D FAPbI₃ perovskite (Figure 9b) and found to endow PSCs with good operational stability against humidity (≈40% RH) (Figure 9c). This 2D perovskite layer can mitigate the ion migration and facilitate the charge transport, as well as consuming the nonperovskite phase of FAPbI₃. It should be pointed out that 2D

perovskite layer can passivate the grain boundary (Figure 9d) and suppress ion migration at the same time. Not limited to that, 2D perovskite can also promote the formation of cubic FAPbI₃ phase during crystallization, thus yielding perovskites with greatly enhanced moisture stability.^[120] In addition to grain boundary passivation and suppression of ion migration, 2D perovskites with alkyl ammonium cations (e.g., tetra-methyl ammonium [TMA], tetra-ethyl ammonium [TEA]) act as a barrier layer hindering the absorption of water molecules on the reactive Pb_{5c} sites and confer perovskite crystals with considerably enhanced moisture resistance. Such improvement is correlated with the bulky hydrophobic ammonium cations and the change of surface of Pb_{5c}–I_{1c} bonds.^[121] More recently, inverted PSCs with 3D/2D heterostructure exhibited extraordinary stability and passed the damp-heat test (85 °C, 85% RH). The nonradiative recombination associated with trap states at perovskite surface is greatly suppressed by 2D perovskite passivation. Notably, the 2D perovskite layer acts as a barrier layer blocking the ingress of oxygen and moisture and concurrent as a defect passivation layer, particularly at elevated temperatures.^[122] Likewise, by gradient dimensionality engineering, Chen et al. incorporated tertiary butyl as spacer cations in 3D perovskites and found that devices with 3D/2D heterojunction endow excellent moisture, thermal, and light stability. Such enhancement of stability is ascribed to the reduced defect density, manifesting the effective defect healing by 2D perovskite layer.^[123] In another case, a localized DJ 2D/3D heterostructure was achieved by partially covering the 3D perovskite surface, which greatly enhances the moisture stability and does not impede the charge transfer. As a result, the

Table 1. Summary of the enhancement of moisture stability by 2D/3D heterostructure.

2D perovskites	Component of 3D perovskites	Moisture stability	Other condition	References
EDBEPbI ₄	MAPbI ₃	>90% of initial PCE, 1000 h, 65% RH	Addition of 2D precursor into 3D precursor	[115]
BAI	FA _{0.83} CS _{0.17} Pb(I _{0.6} Br _{0.4}) ₃	>80% of initial PCE, 1005 h, 45% RH	Addition of 2D precursor into 3D precursor	[118]
4FPEAI	CS _{0.05} (FA _{0.95} MA _{0.05}) _{0.95} Pb(I _{0.95} Br _{0.05}) ₃	>86% of initial PCE, 1080 h, 85% RH >67% of initial PCE, 500 h, 85% RH, 85 °C	Addition of FABr in 2D precursor	[119]
BDAI ₂	FA-based mixed perovskite	>86% of initial PCE, 1300 h, 70% RH >75% of initial PCE, 200 h, 70% RH, 80 °C	Localized 2D/3D heterostructure	[124]
BAI	(FAPbI ₃) _{0.95} (MAPbBr ₃) _{0.05}	>97.3% of initial PCE, 1083 h, 85% RH, RT	Solid-state in-plane growth	[92]
BAI	CS _{0.05} (MA _{0.10} FA _{0.85})Pb(I _{0.90} Br _{0.10}) ₃	>90% of initial PCE, 1000 h, 70 ± 5% RH, 60 ± 5 °C	–	[139]
OLAI	CS _{0.03} (FA _{0.90} MA _{0.10}) _{0.97} PbI ₃	PCE > 19%, 1000 h, 85% RH, 85 °C	–	[122]
DMePDAl ₂	FA _{0.85} MA _{0.1} CS _{0.05} PbI _{2.9} Br _{0.1}	>73% of initial PCE, 740 h, 85% RH	–	[140]
BABr	Rb _{0.05} CS _{0.05} [(FA _{0.83} MA _{0.17})] _{0.9} Pb(I _{0.83} Br _{0.17}) ₃	No PCE degradation, 45 days, 30% RH, dark storage	Thermal annealing after 2D perovskite coated on top of 3D perovskite layer	[141]
BEAI ₂	MAPbI ₃	>85% of initial PCE, 1000 h, 55% RH, dark storage	–	[142]
PYAI	(CS _{0.17} FA _{0.83})Pb(I _{0.8} Br _{0.2}) ₃	>72% of initial PCE, 1000 h, 65% RH, 65 °C	Addition of 2D crystals into 3D precursor	[143]
Gul	FA-based mixed perovskite	>80% of initial PCE, 30 days, 75% RH, dark storage	GuCl bulk incorporation	[144]
TBHCI	FA-based mixed perovskite	>89% of initial PCE, 1656 h, 10–20% RH, RT, dark	–	[123]
XDAI	MAPbI ₃	>80% of initial PCE, 1000 h, 60% RH	Addition of NH ₄ SCN	[145]
CEAI	FA-based mixed perovskite	>98% of initial PCE, 600 h, 40 ± 20% RH, dark	–	[146]

2D/3D devices retain their 86% performance after aging at 70% RH for 1300 h.^[124]

To sum up, 2D perovskites with hydrophobic organic bulky cation are preferentially located at the grain boundary and thus block the moisture permeation because the moisture-induced degradation is mainly initiated at the grain boundary. In addition, 2D perovskite can also reduce the defects such as cationic and halide vacancies, crystal imperfections, etc., which exacerbate the moisture-induced decomposition of perovskites. However, the 2D/3D heterostructure has an adverse impact on the charge extraction due to the poor charge transport cross bulky organic cation as well as the quantum well structure of 2D perovskites.^[125] Therefore, further structural studies of controlling the vertical crystal growth of 2D perovskites are required to achieve well-aligned 2D perovskite and facilitate charge transport.^[126]

3.3. Encapsulation

As a shield of providing an inert and sealed environment and isolating the perovskites from external stimuli, an ideal encapsulant should be endowed with hydrophobicity, low-oxygen permeation, and a benign barrier to volatilization.^[127,128] Encapsulation methods can be classified into two categories, namely, single thin film (STF) and multiple thin film encapsulations (MTF), depending on the film thickness and the number of the barrier layer. Epoxy and polymethyl methacrylate (PMMA), as hydrophobic materials, are suitable for making STF, irrespective of the rigid and flexible substrate.^[129–131] Nevertheless, the poor wettability of hydrophobic materials in turn results in relatively poor adhesion to the substrate, leading to the formation of pinholes.^[132] In addition to the adhesive layers, water can also permeate into perovskites through the sealing materials.^[133] Thereafter, it is of particular significance to further develop new encapsulation materials and methods. For instance, it was found that the phase segregation and species volatilization under oxygen and humidity are suppressed by a solvent-free and low-temperature melting encapsulation method with paraffin as encapsulant.^[134] Notably, the encapsulated device exhibits 1000 h operational lifetime under MPP tracking, as well as good thermal and moisture stability. Another encapsulation method of utilizing the ethylene glycol-induced intermediate layer does not require harsh fabrication conditions and can minimize the damage of plasma-enhanced atomic layer deposition to the PSCs. As a result, the PSCs retained 95% of its initial performance after aging at 80% RH over 2000 h.^[135]

4. Conclusion and Outlook

The instability of perovskites remains a hurdle hindering commercialization despite the great achievement in terms of PCE. In particular, the effect of external stimuli on the perovskite stability should be carefully taken into account when employing photovoltaics in a real-world environment. Thus, understanding the degradation mechanism under different stressors is of utmost significance to enhance the long-term stability of perovskites. We have discussed the positive effects of a certain amount of water on the perovskite film and reviewed the degradation

mechanisms of different perovskites ranging from 3D to 2D under humidity. Accompanied by hydration, disproportionation, and even decomposition, water-induced degradation is found to initiate at the surface and propagate along the grain boundary and in-plane direction, and at last leads to the grain fragmentation. In addition, we unfold the related methods in terms of improving water resistance, particularly forming the 3D/2D heterostructure. The 2D capping layer can, on the one hand, block the water permeation by its hydrophobic bulky organic cation. On the other hand, it can passivate the defects and suppress the ion migration, therefore leading to the enhancement of moisture stability. Among the 3D/2D heterostructures, we highlight the usage of the DJ phase as 2D perovskite layers. The DJ phase has the advantages of structural stability and lattice stiffness compared to the RP phase, arising from stronger hydrogen bonds between the organic spacers and inorganic layers, a shorter interlayer distance between two inorganic layers, and stacked unit cells with perfect alignment. We also highlight the importance of unifying the testing conditions in order to have reproducible and comparable results. In the future, endeavors should be particularly devoted to the encapsulant as well as encapsulation methods.

We expect that 3D/2D heterostructure together with adequate encapsulation methods can effectively mitigate the perovskite instability against humidity.

Acknowledgements

This work was supported by funding from the Deutsche Forschungsgemeinschaft (DFG, German Research Foundation) via Germany's Excellence Strategy—EXC 2089/1—390776260 (e-conversion) and the International Research Training Group 2022 Alberta/Technical University of Munich International Graduate School for Environmentally Responsible Functional Hybrid Materials (ATUMS). The authors acknowledge TUM.solar in the context of the Bavarian Collaborative Research Project Solar Technologies Go Hybrid (SolTech) and the Center for NanoScience (CeNS). K.S. acknowledges the financial support from China Scholarship Council (CSC).

Open Access funding enabled and organized by Projekt DEAL.

Conflict of Interest

The authors declare no conflict of interest.

Keywords

3D/2D heterostructures, degradation mechanisms, moisture stability, perovskites

Received: December 19, 2022

Revised: January 17, 2023

Published online: March 1, 2023

[1] M. Kim, J. Jeong, H. Lu, T. K. Lee, F. T. Eickemeyer, Y. Liu, I. W. Choi, S. J. Choi, Y. Jo, H.-B. Kim, *Science* **2022**, 375, 302.

[2] J. J. Yoo, G. Seo, M. R. Chua, T. G. Park, Y. Lu, F. Rotermund, Y.-K. Kim, C. S. Moon, N. J. Jeon, J.-P. Correa-Baena, *Nature* **2021**, 590, 587.

- [3] H. Min, D. Y. Lee, J. Kim, G. Kim, K. S. Lee, J. Kim, M. J. Paik, Y. K. Kim, K. S. Kim, M. G. Kim, *Nature* **2021**, *598*, 444.
- [4] Q. Jiang, Y. Zhao, X. Zhang, X. Yang, Y. Chen, Z. Chu, Q. Ye, X. Li, Z. Yin, J. You, *Nat. Photonics* **2019**, *13*, 460.
- [5] Y. Zhao, F. Ma, Z. Qu, S. Yu, T. Shen, H.-X. Deng, X. Chu, X. Peng, Y. Yuan, X. Zhang, *Science* **2022**, *377*, 531.
- [6] M. A. Reus, L. K. Reb, A. F. Weinzierl, C. L. Weindl, R. Guo, T. Xiao, M. Schwartzkopf, A. Chumakov, S. V. Roth, P. Müller-Buschbaum, *Adv. Opt. Mater.* **2022**, *10*, 2102722.
- [7] L. K. Reb, M. Böhmer, B. Predeschly, S. Grott, C. L. Weindl, G. I. Ivandekic, R. Guo, C. Dreißigacker, R. Gernhäuser, A. Meyer, *Joule* **2020**, *4*, 1880.
- [8] G. Yang, Z. Ni, Z. J. Yu, B. W. Larson, Z. Yu, B. Chen, A. Alasfour, X. Xiao, J. M. Luther, Z. C. Holman, *Nat. Photonics* **2022**, *16*, 588.
- [9] R. Guo, D. Han, W. Chen, L. Dai, K. Ji, Q. Xiong, S. Li, L. K. Reb, M. A. Scheel, S. Pratap, *Nat. Energy* **2021**, *6*, 977.
- [10] G. Y. Kim, A. Senocrate, T.-Y. Yang, G. Gregori, M. Grätzel, J. Maier, *Nat. Mater.* **2018**, *17*, 445.
- [11] G. Dvitini, S. Cacovici, F. Matteocci, L. Cinà, A. Di Carlo, C. Ducati, *Nat. Energy* **2016**, *1*, 1.
- [12] Y.-H. Seo, J. H. Kim, D.-H. Kim, H.-S. Chung, S.-I. Na, *Nano Energy* **2020**, *77*, 105164.
- [13] K. M. Fransishyn, S. Kundu, T. L. Kelly, *ACS Energy Lett.* **2018**, *3*, 2127.
- [14] M. A. A. Kazemi, N. Folastre, P. Raval, M. Sliwa, J. M. V. Nsanzimana, S. Golonu, A. Demortiere, J. Rousset, O. Lafon, L. Delevoeye, *Energy Environ. Mater.* **2021**, doi: <https://doi.org/10.1002/eem2.12335>.
- [15] J. Huang, S. Tan, P. D. Lund, H. Zhou, *Energy Environ. Sci.* **2017**, *10*, 2284.
- [16] X. Gong, M. Li, X. B. Shi, H. Ma, Z. K. Wang, L. S. Liao, *Adv. Funct. Mater.* **2015**, *25*, 6671.
- [17] X. Yin, Y. Guo, J. Liu, P. Chen, W. Chen, M. Que, W. Que, C. Niu, J. Bian, Y. Yang, *Thin Solid Films* **2017**, *636*, 664.
- [18] M. K. Gangishetty, R. W. Scott, T. L. Kelly, *Nanoscale* **2016**, *8*, 6300.
- [19] K. Meng, C. Wang, Z. Qiao, Y. Zhai, R. Yu, N. Liu, R. Gao, B. Chen, L. Pan, M. Xiao, *Small* **2021**, *17*, 2104165.
- [20] Y. Rong, X. Hou, Y. Hu, A. Mei, L. Liu, P. Wang, H. Han, *Nat. Commun.* **2017**, *8*, doi: [10.1038/ncomms14555](https://doi.org/10.1038/ncomms14555).
- [21] Z. Li, X. Liu, J. Xu, Y. Liao, H. Zhao, B. Zhang, S. F. Liu, J. Yao, *J. Phys. Chem. Lett.* **2019**, *10*, 4587.
- [22] K. Liu, Y. Luo, Y. Jin, T. Liu, Y. Liang, L. Yang, P. Song, Z. Liu, C. Tian, L. Xie, *Nat. Commun.* **2022**, *13*, doi: [10.1038/s41467-022-32482-y](https://doi.org/10.1038/s41467-022-32482-y).
- [23] J. Hidalgo, C. A. Perini, A.-F. Castro-Mendez, D. Jones, H. Köbler, B. Lai, R. Li, S. Sun, A. Abate, J.-P. Correa-Baena, *ACS Energy Lett.* **2020**, *5*, 3526.
- [24] N. Adhikari, A. Dubey, E. A. Gaml, B. Vaagensmith, K. M. Reza, S. A. A. Mabrouk, S. Gu, J. Zai, X. Qian, Q. Qiao, *Nanoscale* **2016**, *8*, 2693.
- [25] H.-H. Huang, Z. Ma, J. Strzalka, Y. Ren, K.-F. Lin, L. Wang, H. Zhou, Z. Jiang, W. Chen, *Cell Rep. Phys. Sci.* **2021**, *2*, 100395.
- [26] J. You, Y. Yang, Z. Hong, T.-B. Song, L. Meng, Y. Liu, C. Jiang, H. Zhou, W.-H. Chang, G. Li, *Appl. Phys. Lett.* **2014**, *105*, 183902.
- [27] B. R. Wygant, G. T. Geberth, A. Z. Ye, A. Dolocan, D. E. Cotton, S. T. Roberts, D. A. Vanden Bout, C. B. Mullins, *ACS Appl. Energy Mater.* **2020**, *3*, 6280.
- [28] X. Li, G. Wu, M. Wang, B. Yu, J. Zhou, B. Wang, X. Zhang, H. Xia, S. Yue, K. Wang, *Adv. Mater.* **2020**, *10*, 2001832.
- [29] X. Guo, Y. Gao, Q. Wei, K. Ho Ngai, M. Qin, X. Lu, G. Xing, T. Shi, W. Xie, J. Xu, *Sol. RRL* **2021**, *5*, 2100555.
- [30] W. Chi, S. K. Banerjee, *Chem. Mater.* **2021**, *33*, 4269.
- [31] N. Z. Koocher, D. Saldana-Greco, F. Wang, S. Liu, A. M. Rappe, *J. Phys. Chem. Lett.* **2015**, *6*, 4371.
- [32] J. S. Yun, J. Kim, T. Young, R. J. Patterson, D. Kim, J. Seidel, S. Lim, M. A. Green, S. Huang, A. Ho-Baillie, *Adv. Funct. Mater.* **2018**, *28*, 1705363.
- [33] P. Toloueinia, H. Khassaf, A. Shirazi Amin, Z. M. Tobin, S. P. Alpay, S. L. Suib, *ACS Appl. Energy Mater.* **2020**, *3*, 8240.
- [34] M. I. Saidaminov, J. Kim, A. Jain, R. Quintero-Bermudez, H. Tan, G. Long, F. Tan, A. Johnston, Y. Zhao, O. Voznyy, *Nat. Energy* **2018**, *3*, 648.
- [35] E. Mosconi, J. M. Azpiroz, F. De Angelis, *Chem. Mater.* **2015**, *27*, 4885.
- [36] Y.-H. Kye, C.-J. Yu, U.-G. Jong, Y. Chen, A. Walsh, *J. Phys. Chem. Lett.* **2018**, *9*, 2196.
- [37] Z. Yang, J. Dou, S. Kou, J. Dang, Y. Ji, G. Yang, W. Q. Wu, D. B. Kuang, M. Wang, *Adv. Funct. Mater.* **2020**, *30*, 1910710.
- [38] R.-Y. Hsu, Y.-J. Liang, Y.-J. Hung, Y.-C. Lin, *Mater. Sci. Semicond. Process.* **2022**, *152*, 107100.
- [39] N. Li, S. Pratap, V. Köstgens, S. Vema, L. Song, S. Liang, A. Davydok, C. Krywka, P. Müller-Buschbaum, *Nat. Commun.* **2022**, *13*, doi: [10.1038/s41467-022-34426-y](https://doi.org/10.1038/s41467-022-34426-y).
- [40] J.-W. Lee, S.-H. Bae, N. De Marco, Y.-T. Hsieh, Z. Dai, Y. Yang, *Mater. Today Energy* **2018**, *7*, 149.
- [41] Q. Wang, B. Chen, Y. Liu, Y. Deng, Y. Bai, Q. Dong, J. Huang, *Energy Environ. Sci.* **2017**, *10*, 516.
- [42] J. Schlipf, L. Bießmann, L. Oesinghaus, E. Berger, E. Metwalli, J. A. Lercher, L. Porcar, P. Müller-Buschbaum, *J. Phys. Chem. Lett.* **2018**, *9*, 2015.
- [43] N. Rolston, K. A. Bush, A. D. Printz, A. Gold-Parker, Y. Ding, M. F. Toney, M. D. McGehee, R. H. Dauskardt, *Adv. Mater.* **2018**, *8*, 1802139.
- [44] C.-J. Tong, W. Geng, Z.-K. Tang, C.-Y. Yam, X.-L. Fan, J. Liu, W.-M. Lau, L.-M. Liu, *J. Phys. Chem. Lett.* **2015**, *6*, 3289.
- [45] J. Yang, B. D. Siempelkamp, D. Liu, T. L. Kelly, *ACS Nano* **2015**, *9*, 1955.
- [46] D. Li, S. A. Bretschneider, V. W. Bergmann, I. M. Hermes, J. Mars, A. Klasen, H. Lu, W. Tremel, M. Mezger, H.-J. R. Butt, *J. Phys. Chem. C* **2016**, *120*, 6363.
- [47] M. Hada, M. Abdullah Al Asad, M. Misawa, Y. Hasegawa, R. Nagaoka, H. Suzuki, R. Mishima, H. Ota, T. Nishikawa, Y. Yamashita, *Appl. Phys. Lett.* **2020**, *117*, 253304.
- [48] A. M. Leguy, Y. Hu, M. Campoy-Quiles, M. I. Alonso, O. J. Weber, P. Azarhoosh, M. Van Schilfgarde, M. T. Weller, T. Bein, J. Nelson, *Chem. Mater.* **2015**, *27*, 3397.
- [49] K. J. Xu, R. T. Wang, A. F. Xu, J. Y. Chen, G. Xu, *ACS Appl. Mater. Interfaces* **2020**, *12*, 48882.
- [50] J. A. Christians, P. A. Miranda Herrera, P. V. Kamat, *J. Am. Chem. Soc.* **2015**, *137*, 1530.
- [51] I. Deretzis, E. Smecca, G. Mannino, A. La Magna, T. Miyasaka, A. Alberti, *J. Phys. Chem. Lett.* **2018**, *9*, 3000.
- [52] C. Zheng, O. Rubel, *J. Phys. Chem. C* **2019**, *123*, 19385.
- [53] M. A. Akhavan Kazemi, P. Raval, K. Cherednichekno, J. N. Chotard, A. Krishna, A. Demortiere, G. M. Reddy, F. Sauvage, *Small Methods* **2021**, *5*, 2000834.
- [54] M. Wu, N. Haji Ladi, Z. Yi, H. Li, Y. Shen, M. Wang, *Energy Technol.* **2020**, *8*, 1900744.
- [55] G. Niu, X. Guo, L. Wang, *J. Mater. Chem. A* **2015**, *3*, 8970.
- [56] W. Xiang, S. F. Liu, W. Tress, *Energy Environ. Sci.* **2021**, *14*, 2090.
- [57] L. K. Ono, E. J. Juarez-Perez, Y. Qi, *ACS Appl. Mater. Interfaces* **2017**, *9*, 30197.
- [58] S. H. Reddy, F. Di Giacomo, A. Di Carlo, *Adv. Mater.* **2022**, *12*, 2103534.
- [59] A. N. Urwick, F. Bastianini, G. E. Pérez, A. Dunbar, *Energy Rep.* **2022**, *8*, 23.

- [60] J. M. Howard, E. M. Tennyson, S. Barik, R. Szostak, E. Waks, M. F. Toney, A. F. Nogueira, B. R. Neves, M. S. Leite, *J. Phys. Chem. Lett.* **2018**, *9*, 3463.
- [61] P. Raval, R. M. Kennard, E. S. Vasileiadou, C. J. Dahlman, I. Spanopoulos, M. L. Chabinye, M. Kanatzidis, G. Manjunatha Reddy, *ACS Energy Lett.* **2022**, *7*, 1534.
- [62] W. Kaiser, D. Ricciarelli, E. Mosconi, A. A. Allothman, F. Ambrosio, F. De Angelis, *J. Phys. Chem. Lett.* **2022**, *13*, 2321.
- [63] R. Chen, Y. Hui, B. Wu, Y. Wang, X. Huang, Z. Xu, P. Ruan, W. Zhang, F. Cheng, W. Zhang, *J. Mater. Chem. A* **2020**, *8*, 9597.
- [64] Z. Lin, Y. Zhang, M. Gao, J. A. Steele, S. Louisia, S. Yu, L. N. Quan, C.-K. Lin, D. T. Limmer, P. Yang, *Matter* **2021**, *4*, 2392.
- [65] S. Dastidar, D. A. Egger, L. Z. Tan, S. B. Cromer, A. D. Dillon, S. Liu, L. Kronik, A. M. Rappe, A. T. Fafarman, *Nano Lett.* **2016**, *16*, 3563.
- [66] J. Lin, M. Lai, L. Dou, C. S. Kley, H. Chen, F. Peng, J. Sun, D. Lu, S. A. Hawks, C. Xie, *Nat. Mater.* **2018**, *17*, 261.
- [67] A. Mattoni, A. Filippetti, C. Caddeo, *J. Phys.: Condens. Matter* **2016**, *29*, 043001.
- [68] Y. Fan, J. Fang, X. Chang, M.-C. Tang, D. Barrit, Z. Xu, Z. Jiang, J. Wen, H. Zhao, T. Niu, *Joule* **2019**, *3*, 2485.
- [69] D. L. Busipalli, K.-Y. Lin, S. Nachimuthu, J.-C. Jiang, *Phys. Chem. Chem. Phys.* **2020**, *22*, 5693.
- [70] T. L. Leung, I. Ahmad, A. A. Syed, A. M. C. Ng, J. Popović, A. B. Djurišić, *Commun. Mater.* **2022**, *3*, doi: 10.1038/s43246-022-00285-9.
- [71] C. Liu, J. Sun, W. L. Tan, J. Lu, T. R. Gengenbach, C. R. McNeill, Z. Ge, Y.-B. Cheng, U. Bach, *Nano Lett.* **2020**, *20*, 1240.
- [72] J. Tang, W. Tian, C. Zhao, Q. Sun, C. Zhang, H. Cheng, Y. Shi, S. Jin, *ACS Omega* **2022**, *7*, 10365.
- [73] A. Dučinskis, G. Y. Kim, D. Moia, A. Senocrate, Y.-R. Wang, M. A. Hope, A. Mishra, D. J. Kubicki, M. Siczek, W. Bury, *ACS Energy Lett.* **2020**, *6*, 337.
- [74] B. Kim, S. I. Seok, *Energy Environ. Sci.* **2020**, *13*, 805.
- [75] Y. Zha, Y. Wang, Y. Sheng, S. Wu, J. Zhang, K. Ma, L. Yang, C. Liu, Y. Di, Z. Gan, *Nanotechnology* **2022**, *33*, 285702.
- [76] J. Schlipf, Y. Hu, S. Pratap, L. Bießmann, N. Hohn, L. Porcar, T. Bein, P. Docampo, P. Müller-Buschbaum, *ACS Appl. Energy Mater.* **2019**, *2*, 1011.
- [77] B. R. Wygant, A. Z. Ye, A. Dolocan, Q. Vu, D. M. Abbot, C. B. Mullins, *J. Am. Chem. Soc.* **2019**, *141*, 18170.
- [78] B. Chen, J. Song, X. Dai, Y. Liu, P. N. Rudd, X. Hong, J. Huang, *Adv. Mater.* **2019**, *31*, 1902413.
- [79] K. Ho, M. Wei, E. H. Sargent, G. C. Walker, *ACS Energy Lett.* **2021**, *6*, 934.
- [80] M. V. Khenkin, E. A. Katz, A. Abate, G. Bardizza, J. J. Berry, C. Brabec, F. Brunetti, V. Bulović, Q. Burlingame, A. Di Carlo, *Nat. Energy* **2020**, *5*, 35.
- [81] B. Kim, M. Kim, J. H. Lee, S. I. Seok, *Adv. Sci.* **2020**, *7*, 1901840.
- [82] F. U. Kosasih, C. Ducati, *Nano Energy* **2018**, *47*, 243.
- [83] J. Schlipf, P. Docampo, C. J. Schaffer, V. Körstgens, L. Bießmann, F. Hanusch, N. Giesbrecht, S. Bernstorff, T. Bein, P. Müller-Buschbaum, *J. Phys. Chem. Lett.* **2015**, *6*, 1265.
- [84] J. Schlipf, P. Müller-Buschbaum, *Adv. Mater.* **2017**, *7*, 1700131.
- [85] M. Qin, P. F. Chan, X. Lu, *Adv. Mater.* **2021**, *33*, 2105290.
- [86] J. Wang, W. Wang, Y. Chen, L. Song, W. Huang, *Small Methods* **2021**, *5*, 2100829.
- [87] S. Pratap, F. Babbe, N. S. Barchi, Z. Yuan, T. Luong, Z. Haber, T.-B. Song, J. L. Slack, C. V. Stan, N. Tamura, C. M. Sutter-Fella, P. Müller-Buschbaum, *Nat. Commun.* **2021**, *12*, doi: 10.1038/s41467-021-25898-5.
- [88] B. Chen, P. N. Rudd, S. Yang, Y. Yuan, J. Huang, *Chem. Soc. Rev.* **2019**, *48*, 3842.
- [89] F. Gao, Y. Zhao, X. Zhang, J. You, *Adv. Mater.* **2020**, *10*, 1902650.
- [90] D. Luo, R. Su, W. Zhang, Q. Gong, R. Zhu, *Nat. Rev. Mater.* **2020**, *5*, 44.
- [91] D. Yu, F. Cao, J. Liao, B. Wang, C. Su, G. Xing, *Nat. Commun.* **2022**, *13*, doi: 10.1038/s41467-022-33752-5.
- [92] Y.-W. Jang, S. Lee, K. M. Yeom, K. Jeong, K. Choi, M. Choi, J. H. Noh, *Nat. Energy* **2021**, *6*, 63.
- [93] L. N. Quan, M. Yuan, R. Comin, O. Voznyy, E. M. Beauregard, S. Hoogland, A. Buin, A. R. Kirmani, K. Zhao, A. Amassian, *J. Am. Chem. Soc.* **2016**, *138*, 2649.
- [94] D. Meggiolaro, S. G. Motti, E. Mosconi, A. J. Barker, J. Ball, C. A. R. Perini, F. Deschler, A. Petrozza, F. De Angelis, *Energy Environ. Sci.* **2018**, *11*, 702.
- [95] M. Ding, L. Sun, X. Chen, T. Luo, T. Ye, C. Zhao, W. Zhang, H. Chang, *J. Mater. Sci.* **2019**, *54*, 12000.
- [96] Q. Tai, P. You, H. Sang, Z. Liu, C. Hu, H. L. Chan, F. Yan, *Nat. Commun.* **2016**, *7*, doi: 10.1038/ncomms11105.
- [97] Z. Zhang, Y. Zhou, Y. Cai, H. Liu, Q. Qin, X. Lu, X. Gao, L. Shui, S. Wu, J.-M. Liu, *J. Power Sources* **2018**, *377*, 52.
- [98] Q. Jiang, D. Rebolgar, J. Gong, E. L. Piacentino, C. Zheng, T. Xu, *Angew. Chem.* **2015**, *127*, 7727.
- [99] Y. Zhang, Y. Ma, I. Shin, Y. K. Jung, B. R. Lee, S. Wu, J. H. Jeong, B. H. Lee, J. H. Kim, K. H. Kim, *ACS Appl. Mater. Interfaces* **2020**, *12*, 7186.
- [100] T. V. Phan Vu, M. T. Nguyen, D. T. T. Nguyen, T. D. Vu, D. L. Nguyen, N. M. An, M. H. Nguyen, C. D. Sai, V. D. Bui, C. H. Hoang, *J. Electron. Mater.* **2017**, *46*, 3622.
- [101] R. Sa, B. Luo, Z. Ma, L. Liang, D. Liu, *J. Solid State Chem.* **2022**, *309*, 122956.
- [102] K.-L. Huang, Y.-H. Chang, P.-Y. Lin, K.-W. Hsu, D. E. Beck, S. Hsieh, *J. Phys. Chem. C* **2022**, *126*, 13441.
- [103] T. Liu, Y. Li, S. Feng, W. Yang, R. Xu, X. Zhang, H. Yang, W. Fu, *ACS Appl. Mater. Interfaces* **2019**, *12*, 904.
- [104] C. Chen, X. Zhuang, W. Bi, Y. Wu, Y. Gao, G. Pan, D. Liu, Q. Dai, H. Song, *Nano Energy* **2020**, *68*, 104315.
- [105] W. Chen, H. Chen, G. Xu, R. Xue, S. Wang, Y. Li, Y. Li, *Joule* **2019**, *3*, 191.
- [106] Y. Sun, Y. Wu, X. Fang, L. Xu, Z. Ma, Y. Lu, W.-H. Zhang, Q. Yu, N. Yuan, J. Ding, *J. Mater. Chem. A* **2017**, *5*, 1374.
- [107] B. Li, C. Fei, K. Zheng, X. Qu, T. Pullerits, G. Cao, J. Tian, *J. Mater. Chem. A* **2016**, *4*, 17018.
- [108] S. Fu, X. Li, J. Wan, W. Zhang, W. Song, J. Fang, *Adv. Funct. Mater.* **2022**, *32*, 2111116.
- [109] S. Tan, J. Shi, B. Yu, W. Zhao, Y. Li, Y. Li, H. Wu, Y. Luo, D. Li, Q. Meng, *Adv. Funct. Mater.* **2021**, *31*, 2010813.
- [110] X. Chang, J. Fang, Y. Fan, T. Luo, H. Su, Y. Zhang, J. Lu, L. Tsetseris, T. D. Anthopoulos, S. Liu, *Adv. Mater.* **2020**, *32*, 2001243.
- [111] D. Wei, H. Huang, P. Cui, J. Ji, S. Dou, E. Jia, S. Sajid, M. Cui, L. Chu, Y. Li, *Nanoscale* **2019**, *11*, 1228.
- [112] S. Fu, W. Zhang, X. Li, J. Guan, W. Song, J. Fang, *ACS Energy Lett.* **2021**, *6*, 3661.
- [113] G. Grancini, M. K. Nazeeruddin, *Nat. Rev. Mater.* **2019**, *4*, 4.
- [114] F. Zhang, H. Lu, J. Tong, J. J. Berry, M. C. Beard, K. Zhu, *Energy Environ. Sci.* **2020**, *13*, 1154.
- [115] P. Li, Y. Zhang, C. Liang, G. Xing, X. Liu, F. Li, X. Liu, X. Hu, G. Shao, Y. Song, *Adv. Mater.* **2018**, *30*, 1805323.
- [116] E. H. Jung, N. J. Jeon, E. Y. Park, C. S. Moon, T. J. Shin, T.-Y. Yang, J. H. Noh, J. Seo, *Nature* **2019**, *567*, 511.
- [117] R. Guo, A. Buyruk, X. Jiang, W. Chen, L. K. Reb, M. A. Scheel, T. Ameri, P. Müller-Buschbaum, *J. Phys.: Energy* **2020**, *2*, 034005.
- [118] Z. Wang, Q. Lin, F. P. Chmiel, N. Sakai, L. M. Herz, H. J. Snaith, *Nat. Energy* **2017**, *2*, doi: 10.1038/nenergy.2017.135.

- [119] M. K. Mohammed, A. E. Shalan, M. Dehghanipour, H. Mohseni, *Chem. Eng. J.* **2022**, 428, 131185.
- [120] J.-W. Lee, Z. Dai, T.-H. Han, C. Choi, S.-Y. Chang, S.-J. Lee, N. De Marco, H. Zhao, P. Sun, Y. Huang, *Nat. Commun.* **2018**, 9, doi: 10.1038/s41467-018-05454-4.
- [121] S. Yang, Y. Wang, P. Liu, Y.-B. Cheng, H. J. Zhao, H. G. Yang, *Nat. Energy* **2016**, 1, doi: 10.1038/nenergy.2015.16.
- [122] R. Azmi, E. Ugur, A. Seitkhan, F. Aljamaan, A. S. Subbiah, J. Liu, G. T. Harrison, M. I. Nugraha, M. K. Eswaran, M. Babics, *Science* **2022**, 376, 73.
- [123] B. Liu, J. Hu, D. He, L. Bai, Q. Zhou, W. Wang, C. Xu, Q. Song, D. Lee, P. Zhao, F. Hao, X. Niu, Z. Zang, J. Chen, *ACS Appl. Mater. Interfaces* **2022**, 14, 21079.
- [124] W. Li, X. Gu, C. Shan, X. Lai, X. W. Sun, A. K. K. Kyaw, *Nano Energy* **2022**, 91, 106666.
- [125] M. A. Mahmud, T. Duong, J. Peng, Y. Wu, H. Shen, D. Walter, H. T. Nguyen, N. Mozaffari, G. D. Tabi, K. R. Catchpole, *Adv. Funct. Mater.* **2022**, 32, 2009164.
- [126] G. Wu, T. Yang, X. Li, N. Ahmad, X. Zhang, S. Yue, J. Zhou, Y. Li, H. Wang, X. Shi, *Matter* **2021**, 4, 582.
- [127] W. Lv, L. Li, M. Xu, J. Hong, X. Tang, L. Xu, Y. Wu, R. Zhu, R. Chen, W. Huang, *Adv. Mater.* **2019**, 31, 1900682.
- [128] Y. Wang, I. Ahmad, T. Leung, J. Lin, W. Chen, F. Liu, A. M. C. Ng, Y. Zhang, A. B. Djurišić, *ACS Mater. Au* **2022**, 2, 215.
- [129] Y. Jiang, L. Qiu, E. J. Juárez-Pérez, L. K. Ono, Z. Hu, Z. Liu, Z. Wu, L. Meng, Q. Wang, Y. Qi, *Nat. Energy* **2019**, 4, 585.
- [130] I. Suárez, E. J. Juárez-Pérez, J. Bisquert, I. Mora-Seró, J. P. Martínez-Pastor, *Adv. Mater.* **2015**, 27, 6157.
- [131] H. C. Weerasinghe, Y. Dkhissi, A. D. Scully, R. A. Caruso, Y.-B. Cheng, *Nano Energy* **2015**, 18, 118.
- [132] A. Uddin, M. B. Upama, H. Yi, L. Duan, *Coatings* **2019**, 9, 65.
- [133] F. Matteocci, L. Cinà, E. Lamanna, S. Cacovich, G. Divitini, P. A. Midgley, C. Ducati, A. Di Carlo, *Nano Energy* **2016**, 30, 162.
- [134] S. Ma, Y. Bai, H. Wang, H. Zai, J. Wu, L. Li, S. Xiang, N. Liu, L. Liu, C. Zhu, *Adv. Mater.* **2020**, 10, 1902472.
- [135] H. Wang, Y. Zhao, Z. Wang, Y. Liu, Z. Zhao, G. Xu, T.-H. Han, J.-W. Lee, C. Chen, D. Bao, *Nano Energy* **2020**, 69, 104375.
- [136] G. Wu, R. Liang, M. Ge, G. Sun, Y. Zhang, G. Xing, *Adv. Mater.* **2022**, 34, 2105635.
- [137] P. Singh, R. Mukherjee, S. Avasthi, *ACS Appl. Mater. Interfaces* **2020**, 12, 13982.
- [138] Y. Liu, S. Akin, L. Pan, R. Uchida, N. Arora, J. V. Milić, A. Hinderhofer, F. Schreiber, A. R. Uhl, S. M. Zakeeruddin, *Sci. Adv.* **2019**, 5, eaaw2543.
- [139] S. Sidhik, Y. Wang, M. De Siena, R. Asadpour, A. J. Torma, T. Terlier, K. Ho, W. Li, A. B. Puthirath, X. Shuai, *Science* **2022**, 377, 1425.
- [140] F. Zhang, S. Y. Park, C. Yao, H. Lu, S. P. Dunfield, C. Xiao, S. Uličná, X. Zhao, L. Du Hill, X. Chen, *Science* **2022**, 375, 71.
- [141] G. Yang, Z. Ren, K. Liu, M. Qin, W. Deng, H. Zhang, H. Wang, J. Liang, F. Ye, Q. Liang, *Nat. Photonics* **2021**, 15, 681.
- [142] D. Lin, T. Zhang, J. Wang, M. Long, F. Xie, J. Chen, B. Wu, T. Shi, K. Yan, W. Xie, *Nano Energy* **2019**, 59, 619.
- [143] M. Xiong, W. Zou, K. Fan, C. Qin, S. Li, L. Fei, J. Jiang, H. Huang, L. Shen, F. Gao, *ACS Energy Lett.* **2022**, 7, 550.
- [144] X. Zhang, W. Zhou, X. Chen, Y. Chen, X. Li, M. Wang, Y. Zhou, H. Yan, Z. Zheng, Y. Zhang, *Adv. Mater.* **2022**, 12, 2201105.
- [145] Yukta, N. Parikh, R. D. Chavan, P. Yadav, M. K. Nazeeruddin, S. Satapathi, *ACS Appl. Mater. Interfaces* **2022**, 14, 29744.
- [146] B. Yang, J. Suo, F. Di Giacomo, S. Olthof, D. Bogachuk, Y. Kim, X. Sun, L. Wagner, F. Fu, S. M. Zakeeruddin, *ACS Energy Lett.* **2021**, 6, 3916.



Kun Sun is presently a Ph.D. student at the School of Natural Sciences, Technical University of Munich, under the supervision of Professor Peter Müller-Buschbaum. His current research is related to the growth of perovskite films and degradation mechanisms of perovskite solar cells.



Peter Müller-Buschbaum is a full professor in the School of Natural Sciences at Technical University of Munich, Germany, heading the Chair of Functional Materials. Moreover, he is the scientific director of the Munich Neutron Source FRM II, scientific director of the Heinz Maier Leibnitz Zentrum MLZ, and heading the Bavarian key lab TUM.solar. His research interests include polymer and hybrid materials for energy and sensing applications with a special focus on thin films and nanostructures, including kinetic, in situ, and operando experiments.